



# The effect of choosing dependent variables and cell-face velocities on convergence of the SIMPLE algorithm using non-orthogonal grids

H. Lai and Y.Y. Yan

*Department of Mechanical and Manufacturing Engineering,  
 Nottingham Trent University, Nottingham, UK*

**Keywords** *Fluid mechanics, Algorithms, Convergence*

**Abstract** *In this paper the effects of choosing dependent variables and cell face velocities on convergence of the SIMPLE algorithm are discussed. Using different velocity components as either dependent variables or cell-face velocities, both convergent rate and calculation accuracy of the algorithm are compared and studied. A novel method, named "cross-correction", is developed to improve the convergence of the algorithm of using non-orthogonal grids. Cases with benchmark and analytical solutions are used for numerical experiments and validation. The results show that, although different velocity components are employed as either dependent variables or cell face velocities, there is no obvious difference in both the convergent rates and numerical solutions. Moreover, the "cross-correction" method is validated by computations with several first-order and high-order convection schemes; and the generality of convergence improvement achieved by the method is shown in the paper.*

## Nomenclature

$A$	= discretisation coefficient in equation (14)	$J^{ij}$	= cofactor of the element in the $i$ th row and $j$ th column in the matrix $(\vec{e}_1, \vec{e}_2, \vec{e}_3)$
$a$	= combined convection-diffusion coefficient in equation (8)	$m$	= mass source term in the pressure correction equations (14) and (20)
$C$	= discretisation coefficient in equation (20)	$P$	= grid node at the centre of control volume
$E_1, E_2, E_3$	= computational errors defined in equation (21)	$p, p^*, p'$	= pressure, initial pressure value and pressure correction
$\vec{e}^i, \vec{e}_i$	= contravariant and covariant bases of curvilinear coordinates	$Q, Q_1$	= flow rates at inlet boundary and cross-section
$\vec{e}_i^o$	= unit vector of $\vec{e}_i$	$\vec{R}$	= position of $P$
$F_i^i$	= convection-diffusion flux	$S(\phi), S'(\phi),$	= source terms related to transport variable $\phi$
$g, g^{ij}, g_{ij}$	= determinant value, contravariant components and covariant components of determinant tensor	$S_{pr}(\phi), \overline{S(\phi)}$	
$\vec{I}_i$	= base vector of Cartesian coordinates	$U^i, u_i$	= contravariant and Cartesian components of velocity $\vec{V}$

$\vec{V}, V_i$	= velocity and its physical covariant component	$\Gamma_{jk}^i$	= the second kind of Christofel sign	Effect of choosing dependent variables
$\vec{V}^*, \vec{V}'$	= initial velocity and velocity correction	<i>Superscripts</i>		
$X, X_{out}$	= horizontal distance from the inlet of Roache's tunnel and its maximum value	$i, j, k$	= free indexes of contravariant component	
$x^j$	= contravariant curvilinear coordinates line	<i>Subscripts</i>		
$y_i$	= Cartesian coordinates line	$i, j, k$	= free indexes of covariant component	
<i>Greek symbols</i>		$NB$	= neighbour points to node, $P$ , i.e. $N, S, E, W$	
$\phi$	= general transport field variables (dependent variable)	$P$	= pertaining to grid point $P$	
$\Gamma_\phi$	= diffusion coefficient of $\phi$	$P + 0.5$	= cell face in the increasing direction of $x^j$ and close to $P$	
		$n, s, e, w$	= pertaining cell faces $n, s, e, w$	

### Introduction

The semi-implicit method for pressure-linked equations (SIMPLE), a well-developed numerical algorithm for pressure-velocity coupling equations, has played an important role in solving fluid flow and heat transfer problems since it was put forward by Patankar and Spalding (1972). In particular, after the concept of “pressure-weighted interpolation” or “momentum interpolation” being proposed by Rhie and Chow (1983), the algorithm becomes much easier to apply in numerical calculation because only one set of grids is required. As the pressure field of fluid flow is implicitly related to Mach number, the SIMPLE algorithm was also improved to be capable of simulating compressible flows; these have been reported by several researchers such as Karki and Patankar (1989), Hah and Krain (1990) and Rhie and Stowers (1988).

However, a popular problem accompanying the application of this algorithm for using strong non-orthogonal body fitted grids is its poor convergent performance. To improve such performance, many studies have attempted to employ different velocity components as dependent variables. For example, Karki and Patankar (1988a, 1988b) and Lee and Chiu (1992) chose the covariant physical components, while Xi *et al.* (1991) and Sharatchandra and Rhode (1994) used the contravariant components as dependent variables. Meanwhile, other investigators tried to obtain a pressure-correction equation in which the coefficient matrix may be stronger in diagonal dominance by using different velocity components at cell faces of control volume. For instance, Karki and Patankar (1988a, 1988b, 1989), Lee and Chiu (1992), and Choi *et al.* (1993a, 1993b) applied physical covariant velocities at cell faces instead of the widely used contravariant components. Indeed, all of these studies have contributed a lot to improving the SIMPLE algorithm and made it more efficient and suitable for solving transport problems of fluid flow and heat transfer. It is noted that, however, there is some confusion about the application of non-orthogonal grids in body fitted co-ordinates over the selections of both dependent variables and cell-face velocities. In terms of confusion over choosing dependant variables, a

good example is the calculations of laminar flow in Roache's tunnel, which was carried out by Karki and Patankar (1988b) and Sharatchandra and Rhode (1994) respectively. Karki and Patankar (1988b) suggested using covariant velocities as dependent variables, while Sharatchandra and Rhode (1994) insisted that contravariant components of velocity should be better. As for the confusion over cell-face velocity selection, Choi *et al.* (1993a, 1993b) believed that physical covariant components are better choices than contravariant components which are commonly used, because this could enhance the diagonal dominance of coefficient matrix of the pressure correction equation and therefore improve the convergence. However, in their paper, the covariant velocity component and the physical covariant component are taken to be the same concept; this is a mistake. In addition to this, the superscripts and subscripts used for tensor indexes are not consistent with the conventional definition.

Therefore, it is necessary to study the effect of choosing different dependent variables and cell-face velocities on convergence of the SIMPLE algorithm. This paper reports recent studies on this subject. Based on the definition of velocity components and derivation of equations for the SIMPLE algorithm in non-orthogonal co-ordinates, detailed comparisons for both convergent rate and numerical accuracy when employing different velocity components as dependent variables are carried out. Following the comparisons, the equivalence of "two pressure correction equations" derived by using contravariant components and physical covariant velocity components at cell faces respectively is studied and validated by numerical experiments. In particular, a novel and effective method is developed to improve the convergence of the SIMPLE algorithm of using non-orthogonal grids; and the method is validated by testing examples.

### Basic equations

To simplify the derivations and comparisons, only two-dimensional flows are considered. For the co-ordinates systems of non-orthogonal  $\{x^i | i = 1, 2, 3\}$  and Cartesian  $\{y_i | i = 1, 2, 3\}$ ,  $x^1$  and  $x^2$  lie in the same plain with  $y_1$  and  $y_2$ , while  $x^3$  and  $y_3$  and  $[(\partial\phi)/(\partial x^3)] = 0$  where  $\phi$  is a general variable of the flow field. Without special declaration, the summation rule of Einstein must be obeyed for all free indexes  $i, j$  and  $k$ . As it has been proved by Peric *et al.* (1988) that there is no difference for the convergence of the SIMPLE algorithm between using staggered and non-staggered grids, only non-staggered grids are used in the present study.

#### *Definition of velocity components*

Considering an arbitrary point  $P$  in the field, the position of  $P$  is  $\vec{R}$  and the velocity at the point is  $\vec{V}$ . The Cartesian components  $u_i$ , contravariant components  $U^i$ , covariant components and physical covariant components  $V_i$  of  $\vec{V}$  are defined respectively as:

$$u_i = \vec{V} \cdot \vec{I}_i, \quad U^i = \vec{V} \cdot \vec{e}^i, \quad U_i = \vec{V} \cdot \vec{e}_i, \quad V_i = \vec{V} \cdot \vec{e}_i^o, \quad (1) \quad \text{Effect of choosing dependent variables}$$

where  $\vec{I}_i$  are unit basic vectors of the Cartesian system;  $\vec{e}_i$  are, the covariant basic vectors;  $\vec{e}^i$  are, the contravariant basic vectors; and  $\vec{e}_i^o$  is, the unit vector of  $\vec{e}_i$ . The relevant formulae between these vectors can be summarised as:

$$\begin{cases} \vec{R} = y_i \vec{I}_i \\ \vec{e}_i = \partial \vec{R} / \partial x^i, & \vec{e}^i = g^{ij} \vec{e}_j \\ g = \det[g_{ij}] = 1 / \det[g^{ij}] \\ g_{ij} = \vec{e}_i \cdot \vec{e}_j, & g^{ij} = \vec{e}^i \cdot \vec{e}^j \\ \vec{e}_i^o = \vec{e}_i / \sqrt{g_{ii}} & \text{(no summation for } i\text{)}. \end{cases} \quad (2)$$

By using equations (1) and (2), the relationships of  $u_i$ ,  $U^i$  and  $V_i$  can be expressed as:

$$U^i = a^{ij} u_j, \quad V_i = b_{ij} u_j, \quad U^i = c^{ij} V_j, \quad (3)$$

where:

$$a^{ij} = J^{ij} / \sqrt{g}, \quad b_{ij} = \partial y_j / \partial x^i / \sqrt{g_{ij}}, \quad \text{and } c^{ij} = g^{ij} \sqrt{g_{ij}}$$

(no summation for both  $i$  and  $j$ ).

$J^{ij}$  is the cofactor of the element in the  $i$ th row and  $j$ th column in the matrix  $(\vec{e}_1, \vec{e}_2, \vec{e}_3)^T$ .

### Discretisation equations

The conservation laws of mass and momentum can be expressed in a general form with a dependent variable  $\phi$  as follows:

$$\nabla \cdot (\vec{V} \phi - \Gamma_\phi \nabla \phi) = S(\phi). \quad (4)$$

By integrating equation (4) over the control volume as shown in Figure 1 (shaded area), we have:

$$F_n - F_s + F_e - F_w = [\sqrt{g} S(\phi)]_P \Delta x^1 \Delta x^2 + S'(\phi), \quad (5)$$

where  $F_n, F_s, F_e$  and  $F_w$  are convection-diffusion fluxes across the four cell faces  $n, s, e$  and  $w$  respectively, and  $S'(\phi)$  represents the diffusion term induced by the non-orthogonal grids. By employing a subscript  $P + 0.5$  to express the cell face in the direction of increasing  $x^j$  and close to the point  $P$ , the fluxes and the cross-diffusion term are then represented respectively as:

$$F_{P+0.5} = \left[ \sqrt{g} \left( U^i \phi - \Gamma_\phi g^{ii} \frac{\partial \phi}{\partial x^i} \right) \right]_{P+0.5} \Delta x^j \quad (6)$$

( $j \neq i$  and no summation for  $i$ ),

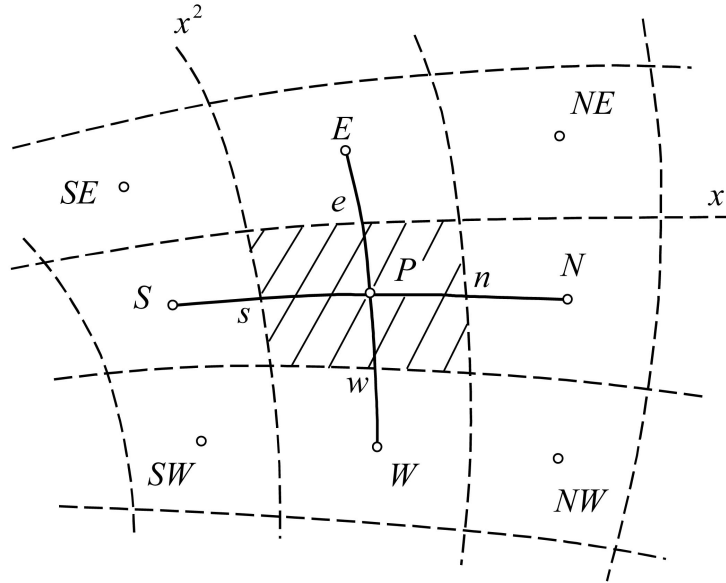


**Figure 1.**  
Control volume  
representation

and

$$S'(\phi) = \left[ \sqrt{g}g^{12} \frac{\partial \phi}{\partial x^2} \Delta x^2 \right]_s^n + \left[ \sqrt{g}g^{21} \frac{\partial \phi}{\partial x^1} \Delta x^1 \right]_w^e. \quad (7)$$

To carry out comparisons, the power-law scheme (Patankar, 1980) is applied to calculate cell-face convection-diffusion fluxes; and the central differencing scheme is employed to determine the derivatives in equation (7). With respect to flow calculations with high order convection schemes, such as Chakravarthy and Osher's (1983) total variation diminishing (TVD) OSHER scheme (second order) and Gaskell and Lau's (1988) SMART scheme (third order), the convection term in equation (6) is calculated using a so-called "deferred correction" method (Khosla and Rubin, 1974), and the high order resolution for non-uniform mesh is guaranteed by the normalised variable and space formulation (NVSF) methodology of Darwish and Moukalled (1994). The final form of the discretised equation is given as:

$$a_P \phi_P = \sum a_{NB} \phi_{NB} + \overline{S(\phi)}, \quad (8)$$

where the subscript *NB* denotes a neighbour point to *P*.

As for momentum equations, the dependent variables  $\phi$  can be any one of  $u_i$ ,  $U^i$  and  $V_i$ , while the coefficients  $a_P$  and  $a_{NB}$  in equation (8) are the same for different  $\phi$ . The  $\overline{S(\phi)}$  in equation (8) consists of the pressure gradient  $S_{pr}(\phi)$ , and an additional term  $S_{ad}(\phi)$ , induced by the non-orthogonal grids. The representations for the source term in equation (8) are given in Table I.

$\phi$	$S_{pr}(\phi)$	$\overline{S(\phi)}$	$S_{ad}(\phi)$	Effect of choosing dependent variables
$u_i$	$-\frac{J^{ji}}{\rho} \frac{\partial p}{\partial x^j} \Delta x^1 \Delta x^2$		$S'(u_i)$	
$U^i$	$-\frac{g^{ij}}{\rho} \frac{\partial p}{\partial x^j} \sqrt{g} \Delta x^1 \Delta x^2$	$\left[ -U^j U^k \Gamma_{jk}^i + \frac{1}{\sqrt{g}} \frac{\partial(\sqrt{g} \Gamma_{\phi} g^{jk} U^m \Gamma_{mk}^i)}{\partial x^j} + \Gamma_{\phi} g^{jk} U_k \Gamma_{jn}^i \right]$	$(\sqrt{g} \Delta x^1 \Delta x^2) + S'(U^i)$	
$V_i$	$-\frac{1}{\rho \sqrt{g_{ij}}} \frac{\partial p}{\partial x^j} \sqrt{g} \Delta x^1 \Delta x^2$ (no summation for $i$ )	$\sum a_{NB} (\check{V}_i = V_i)_{NB} + b_{ij} S'(u_j); (\check{V})_{NB} = (b_{ij})_P (u_j)_{NB}$		

529

**Table I.**  
Formulae of source terms in momentum equation

### Cell-face velocities and pressure-correction equation

A key step of the SIMPLE algorithm is to solve the pressure-correction equation. To avoid calculations of element eliminating for wide band matrix, pressure-correction values at far neighbour nodes (*NE*, *SE*, *NW* and *SW* in Figure 1) to the central node *P* are omitted so that the pressure-correction equation can remain as a five-point scheme for two-dimensional flows.

It is known that the algorithm using strong non-orthogonal grids has poor convergence because an accurate pressure correction for such grids is difficult to obtain. If the diagonal dominance for coefficient matrix of the pressure-correction equation can be enhanced, it will be easier to get an accurate pressure correction, and the convergence of the algorithm is therefore improved. The method of choosing cell face velocities, as indicated by Lee and Chiu (1992) and Choi *et al.* (1993a, 1993b), is concerned with using physical covariant velocities instead of the widely used contravariant components at cell faces to derive “another” pressure-correction equation. However, this method cannot enhance the diagonal dominance for the coefficient matrix of the equation, as the two pressure-correction equations are equivalent. This can be demonstrated in the following paragraphs.

By setting  $\phi = 1$  and  $\Gamma_{\phi} = 0$ , equation (5) becomes continuity and the source term is zero, so:

$$\sqrt{g} U^1 \Delta x^2 \Big|_s^n + \sqrt{g} U^2 \Delta x^1 \Big|_w^e = 0. \quad (9)$$

According to Table I and equation (8), we have:

$$U^i = H^i + B^{ij} \frac{\partial p}{\partial x^j}, \quad (10)$$

where:

$$H^i = \frac{\sum a_{NB} U_{NB}^i + S_{ad}(U^i)}{a_P}, B^{ij} = \frac{-\sqrt{g} g^{ij} \Delta x^1 \Delta x^2}{\rho a_P}.$$

Following the basic steps of the SIMPLE algorithm (see Patankar and

Spalding, 1972), corrections  $U^i$  and  $p'$  are induced to the intermediate values  $U^{i*}$  and  $p^*$  to satisfy both continuity and momentum conservations. The revised parameters of flow are expressed as:

$$U^i = U^{i*} + U^i, \quad p = p^* + p'. \quad (11)$$

Substituting equation (11) into equation (10) and neglecting the effects of pressure correction on  $H^i$  and  $B^{ij}$ , we get:

$$U^i = B^{ij} \frac{\partial p'}{\partial x^j}. \quad (12)$$

To avoid inducing pressure correction at far neighbour nodes, cross derivatives  $[(\partial p')/(\partial x^j)]$  in equation (12) can be dropped, then:

$$U^i = B^{ii} \frac{\partial p'}{\partial x^i} \quad (\text{no summation for } i). \quad (13)$$

Substituting equations (11) and (13) into equation (9) and rearranging terms, a discretisation equation of  $p'$  is obtained as:

$$C_P p'_P = \sum C_{NB} p'_{NB} + m_P, \quad (14)$$

where:

$$C_N = (gg^{11}/\rho a_P)_s (\Delta x^2)^2, \quad C_S = (gg^{11}/\rho a_P)_s (\Delta x^2)^2$$

$$C_E = (gg^{22}/\rho a_P)_e (\Delta x^1)^2, \quad C_W = (gg^{22}/\rho a_P)_w (\Delta x^1)^2$$

$$C_p = \sum C_{NB}$$

$$m_P = \sqrt{g} U^{1*} \Delta x^2 \Big|_n^s + \sqrt{g} U^{2*} \Delta x^1 \Big|_e^w.$$

Equation (14) is the pressure-correction equation derived by using the contravariant components of velocity at the cell faces. As  $C_{NB} > 0$  and  $C_P = \sum C_{NB}$ , the coefficient matrix of equation (14) is already in good diagonal dominance.

Furthermore, if we choose the components of physical covariant velocities,  $V_i$  to calculate the convection at cell faces, "another" pressure correction equation can be derived; this has been indicated by Karki and Patankar (1988a), Lee and Chiu (1992), and Choi *et al.* (1993a, 1993b). That is, according to equation (8) and Table I, we have:

$$V_i = H_i + D_i \frac{\partial p}{\partial x^i} \quad (\text{no summation for } i), \quad (15)$$

where:

$$H_i = \frac{\sum a_{NB} V_{iNB} + S_{ad}(V_i)}{a_P}, \quad D_i = \frac{-\sqrt{g} \Delta x^1 \Delta x^2}{\rho a_P \sqrt{g_{ii}}} \quad (\text{no summation for } i).$$

Effect of choosing  
dependent  
variables

Similar to equations (11) and (12), we have:

$$V_i = V_i^* + V'_i, \quad p = p^* + p', \quad (16)$$

$$V'_i = D_i \frac{\partial p'}{\partial x^i} \quad (\text{no summation for } i). \quad (17)$$

Meanwhile, the substitution of equation (3) into equation (9) yields:

$$\sqrt{g}(c^{11} V_1 + c^{12} V_2) \Delta x^2 \Big|_s^n + \sqrt{g}(c^{21} V_1 + c^{22} V_2) \Delta x^1 \Big|_w^e = 0. \quad (18)$$

By moving the terms  $V_j (j \neq i)$  which are contained in  $x^j$  direction to the right-hand side of equation (18), we obtain:

$$\sqrt{g} c^{11} V_1 \Delta x^2 \Big|_s^n + \sqrt{g} c^{22} V_2 \Delta x^1 \Big|_w^e = m_{no}, \quad (19)$$

where:

$$m_{no} = \sqrt{g} c^{12} V_2 \Delta x^2 \Big|_n^s + \sqrt{g} c^{21} V_1 \Delta x^1 \Big|_e^w.$$

Combining equations (16) and (19) yields “another” pressure-correction equation as:

$$A_P p'_P = \sum A_{NB} p'_{NB} + m_{no} + m_c, \quad (20)$$

where:

$$\begin{aligned} A_N &= (gc^{11} / \sqrt{g_{11}} \rho a_P)_n (\Delta x^2)^2, & A_S &= (gc^{11} / \sqrt{g_{11}} \rho a_P)_s (\Delta x^2)^2 \\ A_E &= (gc^{22} / \sqrt{g_{22}} \rho a_P)_e (\Delta x^1)^2, & A_W &= (gc^{22} / \sqrt{g_{22}} \rho a_P)_w (\Delta x^1)^2 \\ A_P &= \sum A_{NB} \\ m_c &= \sqrt{g} c^{11} V_1^* \Delta x^2 \Big|_n^s + \sqrt{g} c^{22} V_2^* \Delta x^1 \Big|_e^w. \end{aligned}$$

As a result of this, we now seem to have “two” pressure-correction equations. However, using the transformation relationship given in equation (3), it is easy to show:

$$A_P = C_P, \quad m_{no} + m_c = m_P, \quad A_{NB} = C_{NB}.$$

This is to say that pressure-correction equations (14) and (20) are completely equivalent; and using physical covariant components of velocity to replace the



contravariant components at cell faces of control volume cannot get a pressure-correction equation whose diagonal dominance for the coefficients matrix is enhanced.

The above summary is contradictory to the conclusions of Lee and Chiu (1992) and Choi *et al.* (1993a, 1993b). A basic point for the referred works is that the cross derivatives,  $[(\partial p')/(\partial x^j)](j \neq i)$ , are dropped in obtaining equation (13) from equation (12); while the term-dropping actions have not taken place during the derivation of equation (17).

Although such a basic point looks reasonable, by analysis it is not difficult to explain the reason why the terms  $V_j(j \neq i)$ , contained in  $x^j$  direction need to be moved to the right hand of equation (18) in deriving equation (19). In fact, this needs the same consideration of dropping cross derivatives from equation (12). The only aim of these actions is to prevent  $p'$  at far neighbour nodes from appearing in the pressure-correction equation, so that it could be in a format of a five-point scheme (for two-dimensional problems). Such actions are also based on the same assumption that the grids are not strongly non-orthogonal. With the prerequisite destination and assumption, it is impossible to obtain a pressure-correction equation whose coefficient matrix is stronger in diagonal dominance.

#### *The “cross-correction” method*

As indicated before, it is difficult to achieve accurate pressure correction when the numerical grids are strongly non-orthogonal. In such a situation, it will be valuable if the poor convergence of the SIMPLE algorithm can be improved easily and effectively while the five-point scheme for the pressure-correction equation can be retained. In the present study, a novel and effective method is developed.

There are two factors that need to be taken into account. First, although the pressure correction obtained with a five-point scheme in equation (14) or (20) is possibly not as accurate as those achieved with a nine-point scheme in which the  $p'$  at far neighbour nodes is taken into account, it is still a valuable approximation to the accurate  $p'$ . Moreover, the convergent rate is also dependent on the velocity corrections. Based on these considerations, the five-point scheme for the pressure-correction equation is employed to obtain the  $p'$ , but the velocity correction was applied by using equation (12) instead of equation (13). For the case of using physical covariant velocity components at cell faces, the correction for  $V_i$  in  $x^j$  direction can be obtained according to equation (17), meanwhile  $[(\partial p')/(\partial x^j)](j \neq i)$  at the cell face  $P + 0.5$ , was calculated through interpolation between the corresponding values at the nodes  $P$  and  $P + 1$ , and this value was used to get the correction of  $V_j(j \neq i)$ . For simplicity, we name this method “velocity cross-correction” or “cross-correction”.

**Numerical experiment and analysis**

*The convergence of the SIMPLE with different dependent variables*

For convenience of comparison, the contravariant components  $U^i$ , are in the first place employed as cell-face velocities. In this situation, pressure correction can be obtained by equation (14) and the velocity correction can be applied by using equation (17).

*Separated laminar flow in Roache's tunnel.* The separated laminar flow in Roache's tunnel is often employed as a benchmark testing case for numerical algorithms. The benchmark numerical solution for this testing case was reported by Napolitano and Orlando (1985), achieved by Cliffe (cited in Napolitano and Orlando, 1985) using finite element method and with a mesh size  $21 \times 21$  for the calculation. We use this testing case to compare the convergence of the SIMPLE algorithm of using different velocity components as dependent variables in the momentum equations. The flow configuration is shown in Figure 2, and the mesh size in our computation is  $21 \times 20$ , which satisfies the prescribed  $21 \times 21$  grid points requirement for a meaningful comparison for the test problem (Napolitano and Orlando, 1985). Assuming the inflow rate is  $Q$ , and the calculated result for flow rate across a grid line normal to the flow direction is  $Q_1$ , the calculation convergence is declared only after the following error criteria are satisfied:

$$\begin{cases} E_1 = \frac{\max(|Q - Q_1|)}{Q} 10^{-3}, \\ E_2 = \frac{\sum |m_P|}{Q} < 10^{-4} \\ E_3 = \frac{\max(|m_P|)}{Q} < 10^{-6} \end{cases} \quad (21)$$

The results for the case of  $Re = 10$  are shown in Figures 3 and 4. Figure 3 compares the convergent paths of the SIMPLE algorithm, with  $u_i$ ,  $U^i$  and  $V_i$  employed as dependent variables in the momentum equations. The convergent results were also compared with the benchmark solutions in Figure 4. The

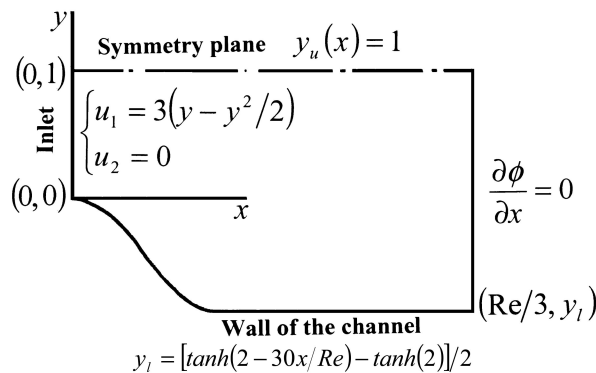
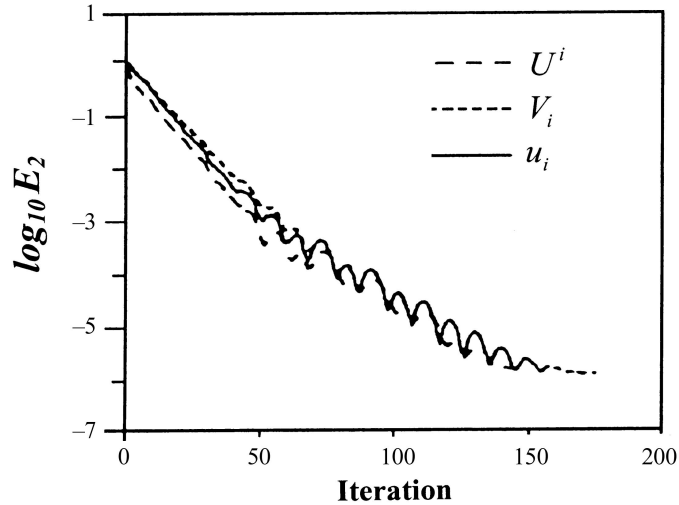


**Figure 2.**  
Flow configuration of  
Roache's tunnel

**Figure 3.**  
Convergence path for  
Roache's tunnel flow –  
choosing dependent  
variables



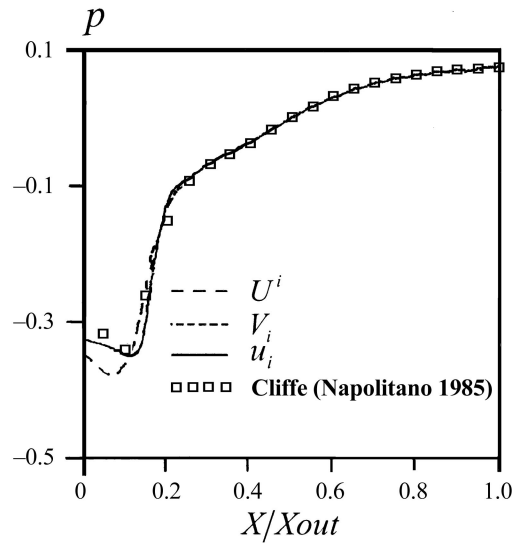
minimum iterations needed to get convergent solutions for  $\phi = u_i$ ,  $U^i$  and  $V_i$  are 90, 91 and 94 respectively (the relaxing factors are  $\alpha_u = 0.7$ ,  $\alpha_p = 0.3$ ). The results indicate that there is no obvious difference in both the convergent rate and the accuracy of the algorithm when different dependent variables in the momentum equations are used.

*Poiseuille flows.* Analytical solutions exist for the Poiseuille flows. In order to examine the effects of non-orthogonal grids on the convergence, the grids system shown in Figure 5 is employed, where  $\beta$  is the angle between non-orthogonal grid lines. The ratio for the length to width of the computational domain is  $L/H = 40$ ; this ensures that the outflow is fully developed, as the Reynolds number is  $Re = 500$  in the calculation.

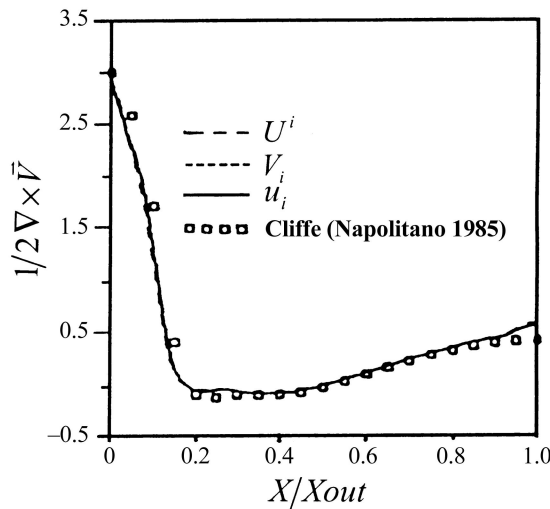
With uniform velocity and pressure imposed at the inlet and outlet boundary, respectively, the analytical solution for the fully developed velocity is  $u_1(y) = u_{1\max}[1 - (y/0.5H)^2]$ , and  $u_2(y) = 0$ ; where  $u_{1\max}$  is the maximum value of the velocity. The error between the computational and analytical solutions is defined as:

$$Err(u_1) = \max\left(\left|\frac{u_{1\text{computational}} - u_{1\text{analytical}}}{u_{1\max}}\right|\right). \quad (22)$$

Figure 6 shows the convergent path for the case of  $\beta = 45^\circ$ . Five cases with  $\beta$  equalling to  $90^\circ$ ,  $60^\circ$ ,  $45^\circ$ ,  $30^\circ$  and  $20^\circ$ , respectively, were calculated. The iterations and final maximum error for the calculations were shown in Table II. Again, the results in Figure 6 and Table II show that the convergent rate of the SIMPLE algorithm does not change with dependent variables, such as  $u_i$ ,  $U^i$  or  $V_i$ , in the momentum equations. Moreover, the error of  $\phi = U^i$  is found to be relatively larger than in the other cases. This may result from error



(a) Pressure at the wall



(b) Vorticity at the wall

**Figure 4.** Computational results of Roache's tunnel flow – choosing dependent variables: (a) pressure at the wall; and (b) vorticity at the wall

accumulation in the integration for the complex source term which contains Christoffel sign.

Based on the above discussions and analysis, it is clear that, in non-orthogonal grids system, the convergence of the SIMPLE algorithm does not change with the choices of velocity components employed as the dependent variable in the momentum equations. To simplify the analysis, only the case of  $\phi = u_i$  will be considered in latter parts of this paper.

*Validation for the equivalence of two pressure-correction equations*

As the test cases are the same as those discussed previously, equations (14) and (20) respectively were employed as a pressure-correction equation in the calculations for comparison. Figures 7 and 8 show the convergent path and the solution respectively for the flow in the Roache's tunnel. The convergent path of Poiseuille flow ( $\beta = 45^\circ$ ) is shown in Figure 9. The results for the cases of  $\beta = 60^\circ, 45^\circ, 30^\circ$  and  $20^\circ$  are also given in Table III.

It can be seen from the two test cases that, when the two pressure-correction equations were employed respectively, the results for both convergent rate and

**Figure 5.**  
Numerical grids for  
computation of  
Poiseuille flow

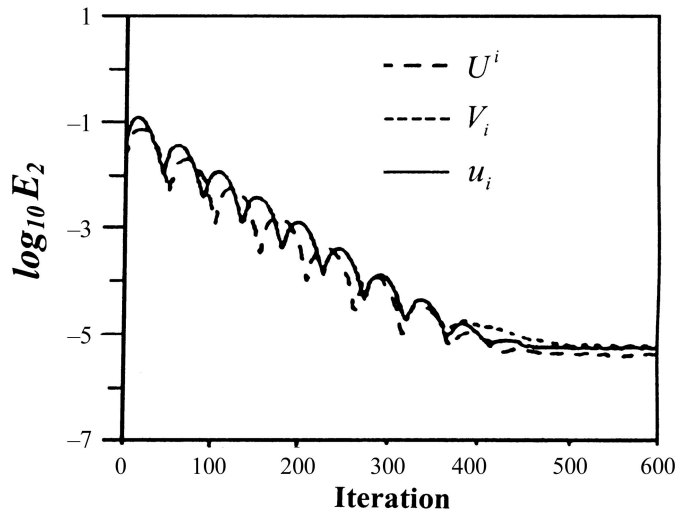
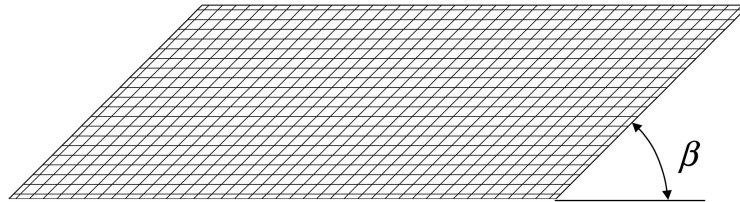


**Figure 6.**  
Convergent path for  
Poiseuille flow ( $\beta = 45^\circ$ )  
– choosing dependent  
variables

$\beta^\circ$	Relax factor ( $\alpha_u, \alpha_p$ )	$E_{rr}(u_1)$ %			Minimum iterations to converge		
		$u_i$	$U^i$	$V_i$	$u_i$	$U^i$	$V_i$
90	0.7, 0.3	0.1312	0.1312	0.1314	185	180	200
60	0.7, 0.3	0.1517	0.1546	0.1521	240	230	255
45	0.6, 0.3	0.1869	0.1920	0.1873	280	295	275
30	0.6, 0.2	0.2326	0.2792	0.2315	440	450	410
30	0.6, 0.3	/	/	/	Divergent	Divergent	Divergent
20	0.6, 0.2	/	/	/	Divergent	Divergent	Divergent
20	0.6, 0.1	0.3418	0.4511	0.3926	700	720	750

**Table II.**  
Convergency of  
SIMPLE for Poiseuille  
flow with different  
dependent variables

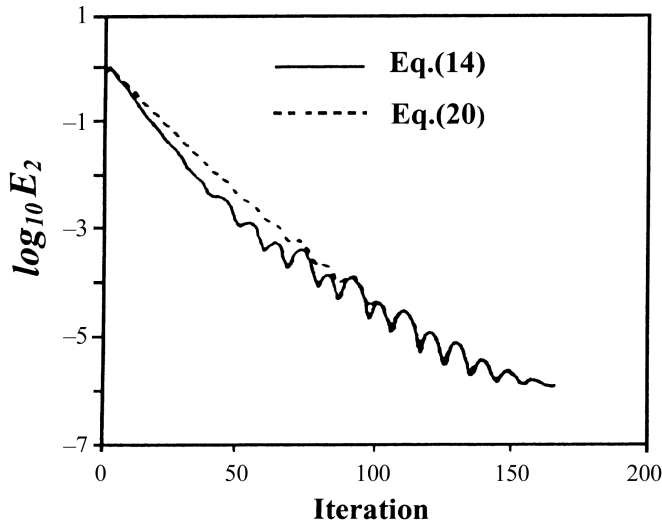


**Figure 7.**  
Convergent path for  
Roache's tunnel flow –  
choosing cell face  
velocity

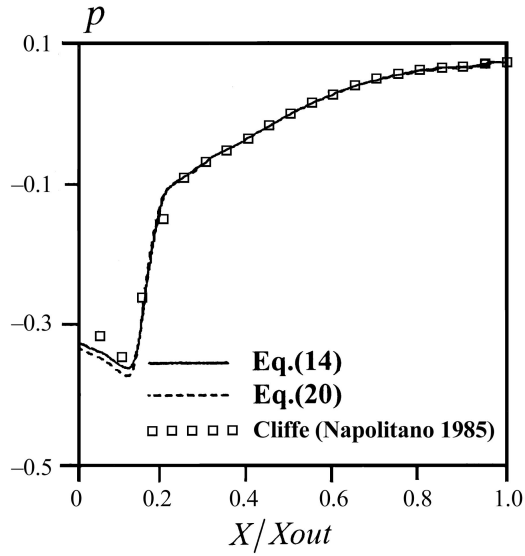
calculation accuracy are very consistent. This indicates that the convergence of the SIMPLE algorithm hardly changes with the choices of cell-face velocities; and the equivalence of equations (14) and (20) is effectively validated.

*Effects of “cross-correction” on convergence*

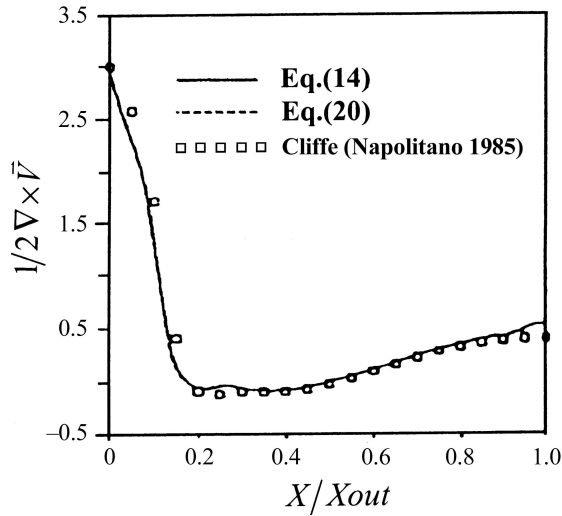
The effect of cell-face velocity cross-correction on convergence is validated in two steps. One is to calculate convection by using the widely-used power law. The other is to examine the results of calculations of using different convection schemes. For convenience, the term of cell-face velocity cross-correction is briefly referred as “cross-correction” and that obtaining cell-face velocity corrections with equation (13) or (17) is referred as “original”.

*Calculations of using power law.* The convergent paths of numerical simulations for flow in Roache's tunnel are shown in Figure 10. These results are achieved by using two different methods of cell-face velocity correction, respectively. The results for Poiseuille flow are presented in Figure 11 ( $\beta = 45^\circ$ ) and Table IV (The corresponding results of “original” are the same as those in Table III and are therefore omitted).

The comparisons for convergent paths given in Figures 10 and 11 indicate that the effects of the “cross-correction” method on the convergence acceleration are significant. Typically, by using such cell-face velocity “cross-correction” method, the number of iterations for a convergent solution is largely reduced. It should be pointed out that, for Poiseuille flow, Table IV shows that the “cross-correction” is only effective for some conditions. For example, convergence is accelerated for  $\beta = 60^\circ$ ,  $45^\circ$  and  $30^\circ$ ; but for  $\beta = 90^\circ$ , the grid lines are orthogonal and the “cross-correction” method becomes invalid; for  $\beta = 20^\circ$ , the grids are strongly non-orthogonal, the effect of “cross-correction” is not



(a) Pressure at the wall



(b) Vorticity at the wall

**Figure 8.**  
Computational results of  
Roache's tunnel flow –  
choosing cell-face  
velocity

---

significant, because the pressure corrections obtained by five-point schemes are far away from the accurate value of  $p'$ .

*Comparison for different convection schemes.* The “cross-correction” is effective in accelerating the convergence of calculations with different convection schemes. This can be shown in the following comparisons.

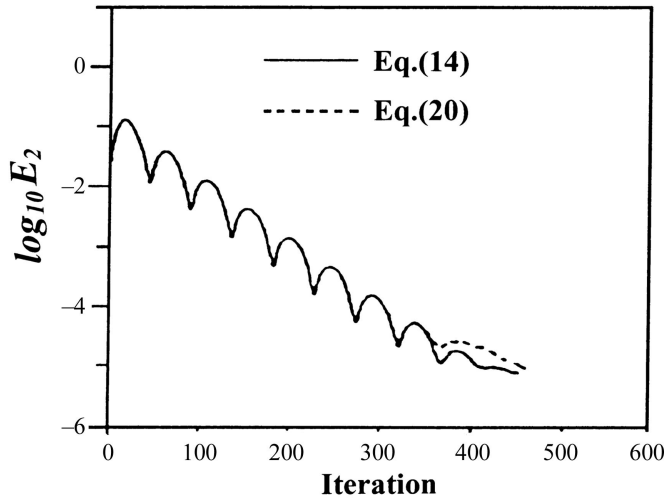


**Figure 9.**  
Convergent path for Poiseuille flow ( $\beta = 45^\circ$ ) – choosing cell-face velocity

$\beta^\circ$	Relaxing factor ( $\alpha_u, \alpha_p$ )	$E_{rr}(u_1)$ %		Minimum iterations to converge	
		Equation (14)	Equation (20)	Equation (14)	Equation (20)
60	0.7, 0.3	0.1517	0.1520	240	242
45	0.6, 0.3	0.1869	0.1877	280	283
30	0.6, 0.2	0.2326	0.2321	440	429
20	0.6, 0.1	0.3418	0.3415	700	712

**Table III.**  
Convergency of SIMPLE for Poiseuille flow using different pressure-correction equation

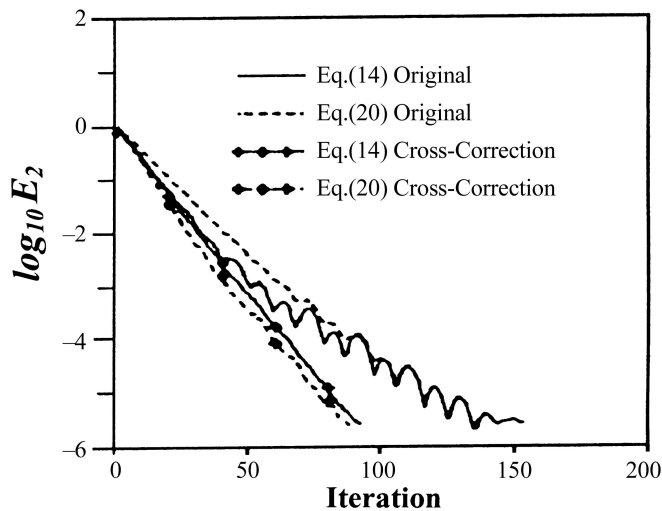


**Figure 10.**  
Effects of "cross-correction" on the convergent path of Roache's tunnel flow



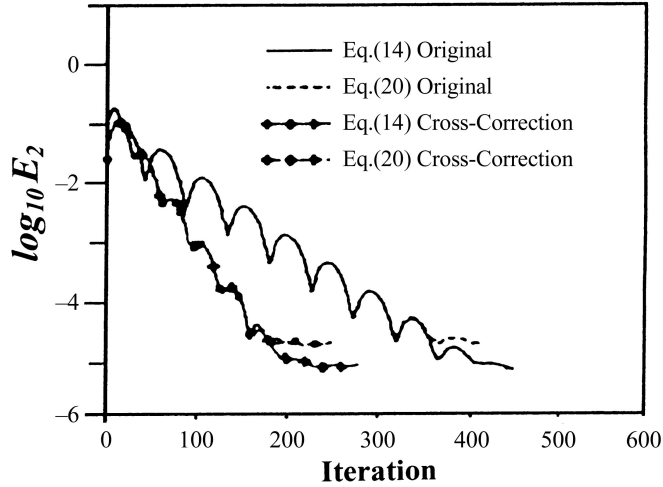


**Figure 11.**  
Effects of  
“cross-correction” on the  
convergent path of  
Poiseuille flow ( $\beta = 45^\circ$ )

$\beta^\circ$	Relaxing factor ( $\alpha_u, \alpha_p$ )	$E_{rr}(u_1)$ %		Minimum iterations to converge	
		Equation (14) cross-section	Equation (20) cross-correction	Equation (14) cross-correction	Equation (20) cross-correction
90	0.7, 0.3	0.1312	0.1311	185	188
60	0.7, 0.3	0.1520	0.1531	198	203
45	0.6, 0.3	0.1855	0.1858	182	180
30	0.6, 0.2	0.2300	0.2324	235	254
20	0.6, 0.1	0.3412	0.3419	620	625

**Table IV.**  
Effects of a  
“cross-correction” for  
Poiseuille flow

The testing example is the lid-driven flow in a cavity with inclined side walls, which is set up as the first test case for non-orthogonal grids by Demirdzic *et al.* (1992). The geometry and boundary conditions are shown in Figure 12, in which the inclination angle  $\beta = 45^\circ$ , and  $L = 1$ , density  $\rho = 1$  and lid velocity  $U_L = 1$ . The Reynolds number, defined using the lid velocity,  $U_L$ , and cavity length,  $L$ , is 1,000 by setting the viscosity to be 0.001. Demirdzic *et al.* (1992) proved that it is possible to obtain a grid-dependent solution if the mesh is coarser than  $50 \times 80$ . They provided a set of benchmark solutions on an extremely fine mesh,  $320 \times 320$ , and a high order convection scheme was applied.

In the present calculation, a non-uniform mesh of  $160 \times 160$ , which expands symmetrically towards the centrelines (CL1 and CL2 in Figure 12) from all walls, is found to be fine enough to obtain the grid-independent solution and is therefore adopted. We have also tried to further refine the mesh to  $320 \times 320$ , similar to what Demirdzic *et al.* (1992) did; however, no further accuracy improvement was achieved.

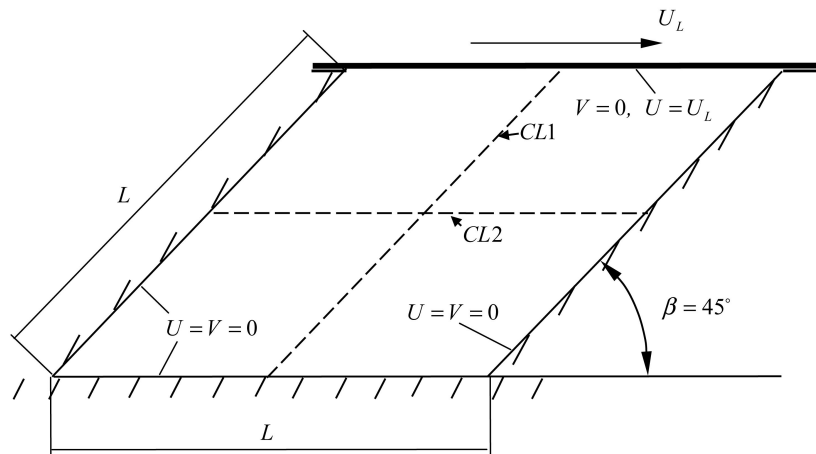


**Figure 12.** Geometry and boundary conditions for squeezed lid-driven cavity flow

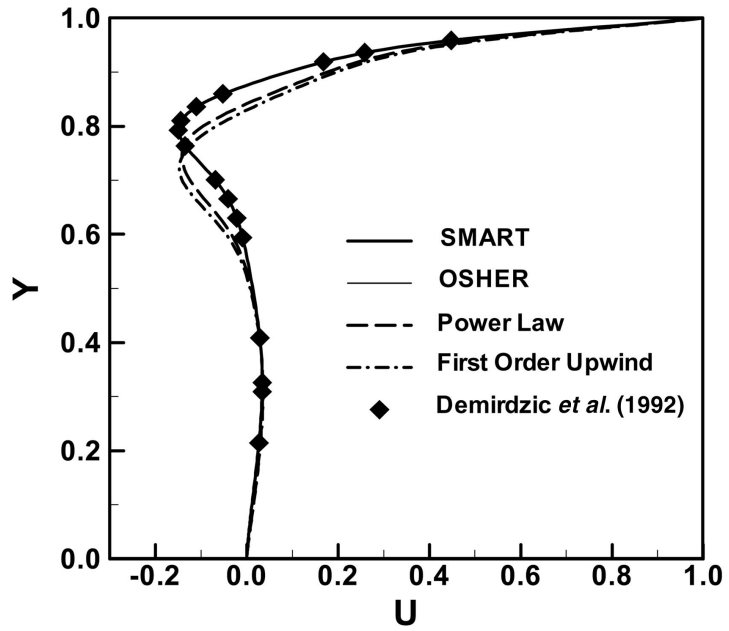
To check the effects of “cross-correction” on convergence improvement, following convection schemes, namely, the first-order upwind scheme, the power-law (which is also of first-order resolution), the second-order TVD scheme OSHER (Chakravarthy and Osher, 1983), and the third-order scheme SMART (Gaskell and Lau, 1988), were employed. To simplify the comparison, only Cartesian velocity components are used as dependent variables, and only equation (14) is employed to obtain pressure correction  $p'$ . As for the relaxation factors for velocity and pressure, they are simply set to be  $\alpha_u = 0.7$  and  $\alpha_p = 0.3$ . The computational results are presented in Figures 13 and 14, respectively.

The profiles of Cartesian velocity components, in horizontal and vertical positions, along centre lines are shown in Figures 13(a) and 13(b). The results for using different convection schemes are compared with the benchmark solutions (Demirdzic *et al.*, 1992). It is noted that first-order schemes (the first-order upwind and the power law) give worse results, while high order schemes (the OSHER and the SMART) offer excellent agreements with the benchmark solution.

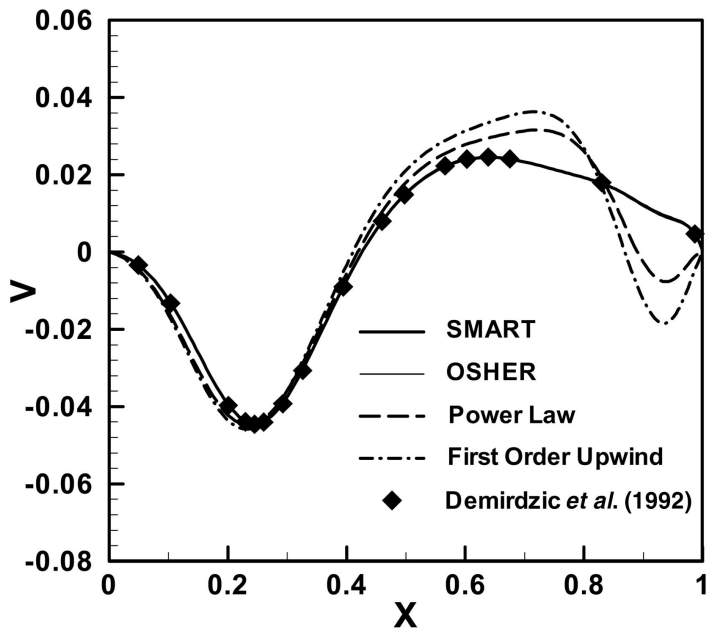
In Figures 14(a)-(d), convergent paths of calculations using the above-mentioned schemes, with and without employing the “cross-correction”, are described. As the flow configuration is an enclosure, the reference flow rate,  $Q$  in equation (21), is calculated by  $Q = \frac{1}{2} U_L \times L$  to define the error criteria. Although the numerical accuracy for different schemes is different, the effect of “cross-correction” on converge acceleration is obvious. In other words, for a certain convection scheme employed, the calculation with “cross-correction” obtains a faster convergence than without “cross-correction”.

## Conclusions

In this paper, the convergence performance of the SIMPLE algorithm of using non-orthogonal grids is studied. The effects of choosing different velocity components as dependent variables on the convergence of calculations are analysed. The equivalence of the two pressure-correction equations derived by



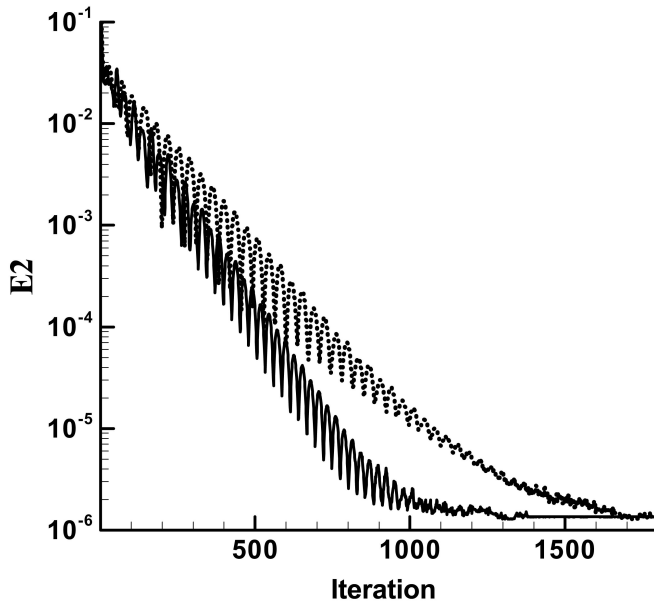
(a)  $U$  – component



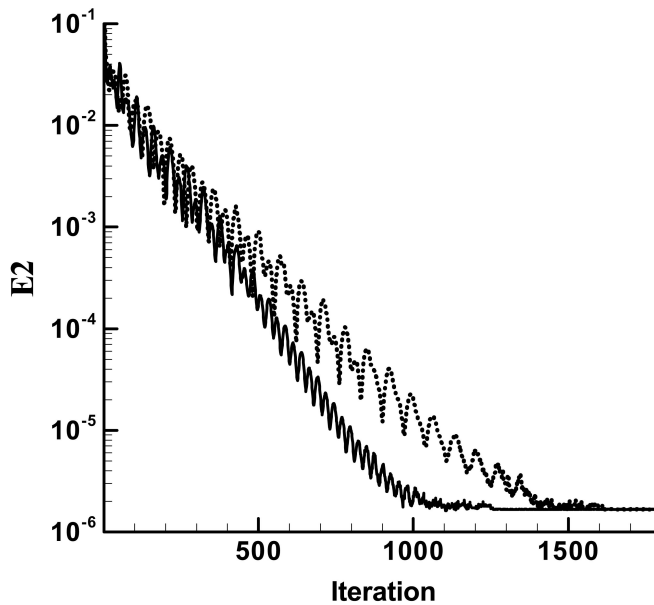
(b)  $V$  – component

**Figure 13.**  
Centreline velocity  
profiles in the squeezed  
cavity: (a)  $U$ -component;  
and (b)  $V$ -component

---



(a) First-order upwind scheme



(b) Power-law

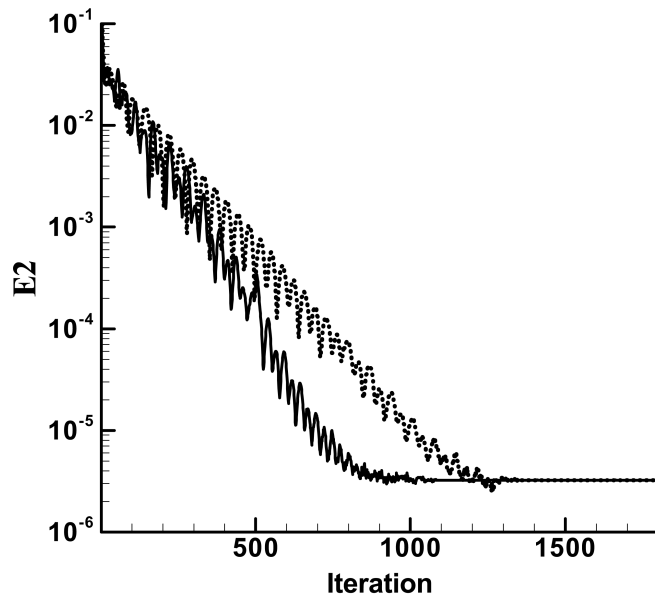
..... Eq.(14) Original  
———— Eq.(14) Cross-Correction

**Figure 14.**  
Convergent paths of  
calculation with and  
without  
“cross-correction”  
*(continued)*

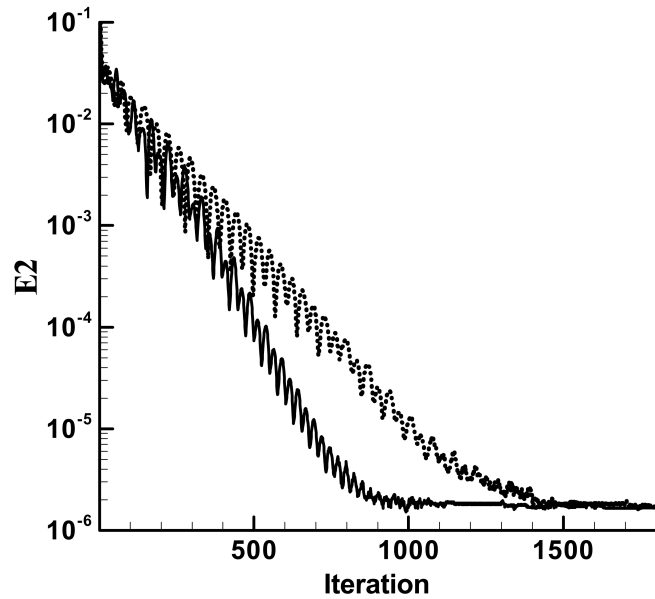
HFF  
11,6

544

---



(c) TVD scheme OSHER



(d) Third-order scheme SMART

Figure 14.

---

..... Eq.(14) Original  
———— Eq.(14) Cross-Correction

---

choosing two kinds of cell-face velocities is demonstrated and numerically validated. A novel method called “cell-face velocity cross-correction” is developed to accelerate the convergence of calculations. The following conclusions can be summarised:

- With non-orthogonal grids, the convergence of the SIMPLE algorithm does not change with dependent variables. Considering the source term for  $\phi = u_i$  being the simplest,  $u_i$  should be suggested for use as a dependent variable in the momentum equations.
- The two pressure-correction equations, derived by using contravariant or physical covariant components of velocity at cell faces respectively, are equivalent. With the prerequisite assumption of grids not being strongly non-orthogonal to keep a five-point scheme, it is impossible to derive a pressure-correction equation whose coefficients matrix is stronger in diagonal dominance.
- The method of cell-face velocity “cross-correction” is effective in improving the convergence of the SIMPLE algorithm of using non-orthogonal grids. However, the method will become less effective if the grids are strongly non-orthogonal because the pressure correction obtained with the five-point scheme will be far away from their accurate values.
- The “cross-correction” method is effective for both first-order and high-order calculations.

### References

- Chakravarthy, S.R. and Osher, S. (1983), “High resolution applications of OSHER upwind scheme for Euler equations”, *AIAA Paper 83-1943*.
- Choi, S.K., Nam, H.Y. and Lee, Y.B. (1993a), “An efficient three-dimensional calculation procedure for incompressible flows in complex geometry”, *Numerical Heat Transfer, Ser. B Vol. 23*, pp. 387-400.
- Choi, S.K., Nam, H.Y. and Nam, C. (1993b), “Use of the momentum interpolation method for numerical solution of incompressible flows in complex geometries: choosing cell face velocities”, *Numerical Heat Transfer, Ser. B Vol. 23*, pp. 21-41.
- Darwish, M.S. and Moukalled, F.M. (1994), “Normalized variable and space formulation methodology for high-resolution schemes”, *Numerical Heat Transfer, Part B, Vol. 26*, pp. 79-96.
- Demirdzic, I., Lilek, Z. and Peric, M. (1992), “Fluid flow and heat transfer test problems for non-orthogonal grids: benchmark solutions”, *International Journal for Numerical Methods in Fluids*, Vol. 15, pp. 329-54.
- Gaskell, P.H. and Lau, A.K.C. (1988), “Curvature compensated convective transport: SMART, a new boundedness preserving transport algorithm”, *International Journal for Numerical Methods in Fluids*, Vol. 8, pp. 617-41.
- Hah, C. and Krain, H. (1990), “Secondary flows and vortex motion in high efficiency back-swept impeller at design and off-design conditions”, *ASME Journal of Turbomachinery*, Vol. 112, No. 1, pp. 7-13.

- Karki, K.C. and Patankar, S.V. (1988a), "Calculation procedure for viscous incompressible flow in complex geometries", *Numerical Heat Transfer*, Vol. 14, pp. 295-307.
- Karki, K.C. and Patankar, S.V. (1988b), "Solution of some two-dimensional incompressible flow problems using a curvilinear coordinate system based calculation procedure", *Numerical Heat Transfer*, Vol. 14, pp. 309-21.
- Karki, K.C. and Patankar, S.V. (1989), "Pressure based calculation procedure for viscous flow at all speeds in arbitrary configurations", *AIAA Journal*, Vol. 27 No. 9, pp. 1167-74.
- Khosla, P.K. and Rubin, S.G. (1974), "A diagonal dominant second-order accurate implicit scheme", *Computers and Fluids*, Vol. 2, pp. 207-9.
- Lee, D. and Chiu, J.J. (1992), "Covariant velocity-based calculation procedure with nonstaggered grids for computation of pulsatile flows", *Numerical Heat Transfer*, Ser. B Vol. 21, pp. 269-86.
- Napolitano, M. and Orlando, P. (1985), "Laminar flow in complex geometry: a comparison", *International Journal for Numerical Methods in Fluids*, Vol. 5, pp. 667-83.
- Patankar, S.V. (1980), *Numerical Heat Transfer and Fluid Flow*, Hemisphere Publishing Corporation, Washington, DC.
- Patankar, S.V. and Spalding, D.B. (1972), "A calculation procedure for heat, mass and momentum transfer in three-dimensional parabolic flows", *Int. Heat and Mass Transfer*, Vol. 115, pp. 1787-1803.
- Peric, M., Kessler, R. and Scheuerer, G. (1988), "Comparison of finite volume numerical methods with staggered and collocated grids", *Computers and Fluids*, Vol. 16, pp. 389-403.
- Rhie, C.M and Chow, W.L. (1983), "Numerical study of the turbulent flow past an airfoil with trailing edge separation", *AIAA Journal*, Vol. 21 No. 11, pp. 1523-32.
- Rhie, C.M. and Stowers, S.T. (1988), "Navier-Stokes analysis for high speed flows using a pressure correction algorithm", *AIAA Journal of Propulsion and Power*, pp. 564-70.
- Sharatchandra, M.C. and Rhode, D.L. (1994), "A new strongly conservative finite volume formulation for fluid flows in irregular geometries using contravariant velocities components", *Numerical Heat Transfer*, Ser. B Vol. 26, pp. 39-62.
- Xi, G., Wang, S. and Miao, Y. (1991), "A calculation for three-dimensional turbulent flow in a centrifugal impeller with any blade geometry", ASME paper 91-GT-171.